Optica Applicata, Vol. XLVIII, No. 1, 2018
DOI: 10.5277/oa180110

Modeling of diffraction radiation processes on periodic metal-dielectric structures in millimeter wavelength range

Oleksandr RYBALKO[1*], Vjacheslav ZHURBA[2], Mykhaylo PETROVSKYI[2], Iuliia RYBALKO[2, 3], Iryna BURIAK[2], Gennadiy VOROBYOV[2]

[1]Department of Electrical Engineering, Technical University of Denmark, DK-2800, Kgs., Lyngby, Denmark

[2]Sumy State University, Rimskiy-Korsakov St. 2, 4007, Sumy, Ukraine

[3]Faculty of Science, University of Porto, 4169-007 Porto, Portugal

[*]Corresponding author: rybalko@elektro.dtu.dk

A general approach to experimental modeling of Cherenkov and diffraction radiation in vacuum electron devices employing periodic metal-dielectric structures is presented. The potential benefits and drawbacks of this approach to the design of microwave devices are discussed. The approach is based on resemblance of electromagnetic properties between the modulated electron beam and the surface wave in a dielectric waveguide. A dedicated millimeter-wave experimental setup is developed and constructed.

Keywords: diffraction radiation, metal-dielectric structure, microwave, waveguide.

1. Introduction

The research in vacuum electronics focuses mainly on the high power tubes development [1, 2] even though there are many applications, such as, for example, spectroscopy, satellite applications, communications and radio-astronomy, where low power devices are required. Such applications usually use signal sources based on solid state devices due to a compact size, light weight, and low power consumption even though they provide low output power. Effective narrow band varactor frequency multipliers have already been constructed up to 2.2 THz, while the experimental results of novel types of varactors are yet only promising [3]. For example, the output power of 2 THz sources does not exceed even several tens of milliwatt.

Vacuum electronics could become an alternative competitive technology. This, however, requires low voltage signal sources development, which could be achieved implementing planar metal-dielectric structures [4]. Such structures analysis is quite complicated due to their specific properties related to excitation of Cherenkov and dif-

fraction radiation [5] with a wide spectrum of spatial harmonics. The same issue in sense of analysis has multilayered metal-dielectric nanofilms [6]. To this end, a general theoretical and experimental methodology development to analyze electromagnetic properties of metal-dielectric structures is required [7].

This paper describes the methodology for identification of modeling regimes for Cherenkov and diffraction radiation. The diffraction radiation processes modeling is realized using methodology described in [8] and tested using a millimeter wave experimental setup. Unlike in the numerical analysis, the suggested approach allows to consider all physical process (the object of investigation is a real device prototype, not a numerical model) which can be observed on real systems of such complicated configuration (contains many periodic, multi-coupled metal-dielectric or resonance structures). In such conditions to set up the integral equations, will create a lot of difficulties. On the contrary, experimental measurements allow the researcher to obtain precise electrodynamic characteristics fast and relatively easy. The measured data is then compared with the results obtained from simulations. The practical aspects of metal-dielectric structures fabrication and implementation in low voltage vacuum devices are discussed in the last section of the paper.

2. Objects of research

The approach of resemblance of electromagnetic properties between the modulated electron beam and dielectric waveguide has been used in the current paper. Based on that, let us start from the theoretical formulation of the problem and continue with the approach on which the idea based. The system scheme based on the metal-dielectric structure is shown in Fig. 1.

Planar electrodynamic system formed by surface $z = -a$ of the strip periodic structure (l – period, d – strips width) on the dielectric layer. Modulated monochromatic electron beam moves close to the metal-dielectric structure with the volume oscillator charge density $\rho = \rho_0 \delta(z - a)\exp[i(ky - \omega t)]$, where: ρ_0 – amplitude of the volume charge

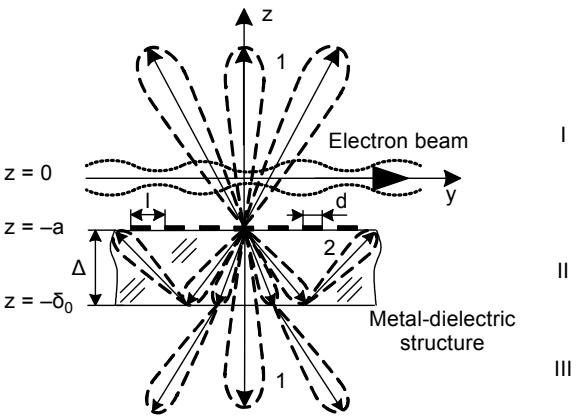

Fig. 1. Model of excitation of diffraction-Cherenkov radiation by an electron beam.

density, $\delta(z-a)$ – delta-function, $\Delta = (\delta_0 - a)$ – width of dielectric with permittivity ε, $k = \omega/v_0$ – wave number, ω – radiation frequency, v_0 – initial electron velocity. Electromagnetic field in areas I ($z > -a$), II ($-\delta_0 < z < -a$), III ($z < -\delta_0$) is as follows:

$$\mathbf{H}^{\mathrm{I}} = \mathbf{H}_{\mathrm{c}} + \mathbf{i}\sum_n A_n \exp\left[iq_n(z+a)\right]\exp(ik_n y) \tag{1}$$

$$\mathbf{H}^{\mathrm{II}} = \mathbf{i}\sum_n \left\{C_n \exp\left[-iq_{n\varepsilon}(z+a)\right] + D_n \exp\left[iq_{n\varepsilon}(z+\delta_0)\right]\right\}\exp(ik_n y) \tag{2}$$

$$\mathbf{H}^{\mathrm{III}} = \mathbf{i}\sum_n F_n \exp\left[-iq_n(z+\delta_0)\right]\exp(ik_n y) \tag{3}$$

$$\mathbf{E}^{\mathrm{I}} = \mathbf{E}_{\mathrm{c}} + \sum_n \left(-\mathbf{j}\sqrt{1-\tau_n^2} + \mathbf{k}\tau_n\right) A_n \exp\left[iq_n(z+a)\right]\exp(ik_n y) \tag{4}$$

$$\mathbf{E}^{\mathrm{II}} = \sum_n \left\{\left(\mathbf{j}\frac{\sqrt{\varepsilon-\tau_n^2}}{\varepsilon} + \mathbf{k}\frac{\tau_n}{\varepsilon}\right) C_n \exp\left[-iq_{n\varepsilon}(z+a)\right]\right.$$

$$\left. + \left(-\mathbf{j}\frac{\sqrt{\varepsilon-\tau_n^2}}{\varepsilon} + \mathbf{k}\frac{\tau_n}{\varepsilon}\right) D_n \exp\left[iq_{n\varepsilon}(z+\delta_0)\right]\right\}\exp(ik_n y) \tag{5}$$

$$\mathbf{E}^{\mathrm{III}} = \sum_n \left(\mathbf{j}\sqrt{1-\tau_n^2} + \mathbf{k}\tau_n\right) F_n \exp\left[-iq_n(z+\delta_0)\right]\exp(ik_n y) \tag{6}$$

where A_n, C_n, D_n, F_n – Fourier components of the diffraction field, and

$$\mathbf{H}_{\mathrm{c}} = \mathbf{i}\beta F \operatorname{sign}(z)\exp(-q|z| + iky) \tag{7}$$

denotes electron beam eigenfield in free space,

$$\mathbf{E}_{\mathrm{c}} = \left[-\mathbf{j}i\theta + \mathbf{k}\operatorname{sign}(z)\right]F\exp(-q|z|)\exp(iky) \tag{8}$$

denotes electron beam proper fields in free space,

$$k_n = k + \frac{2\pi n}{l}, \qquad n = 0, \pm 1, \pm 2, \ldots \tag{9}$$

denotes spatial harmonic number,

$$q = k\theta = k\sqrt{1-\beta^2} \tag{10}$$

$$q_n = k\theta_n = k\beta\sqrt{1-\tau_n^2} \tag{11}$$

$$q_{n\varepsilon} = k\theta_{n\varepsilon} = k\beta\sqrt{\varepsilon-\tau_n^2} \tag{12}$$

$$\tau_n = \frac{\eta + n}{\kappa} \tag{13}$$

and $F = 2\pi\rho_0$, $\beta = \upsilon_0/c$ – normalized electron beam velocity, c – light velocity, $\eta = \kappa/\beta$, $\kappa = l/\lambda$, and λ – radiation wavelength.

Depending on parameters κ, β, and ε, electromagnetic fields in Eqs. (1)–(6) consist of radiated spatial and surface harmonics. Unknown Fourier components of the diffraction radiation, which are field surface harmonics amplitudes, can be found by solving an electrodynamic problem in given current approximation. These harmonics satisfy the accurate boundary conditions on the dielectric surface and Leontovich boundary conditions on the metal surface as well. Electron beam eigenfield with its constant motion velocity υ_0 is a heterogeneous plane wave. Such waves can be formed by a transmission line as the plane dielectric waveguide with propagating E-wave [9, 10].

The approach based on resemblance of electromagnetic properties between the modulated electron beam and the surface wave in a dielectric waveguide [11] has been used in the current research. Similarly to the above-described technique, the scattered field structure as the Fourier components of body and surface wave amplitudes is defined for the electron beam radiation source. The field structure defining methods is based on solving a problem in a given dielectric waveguide field approximation using strict diffraction theory method.

The scattering systems general theoretical analysis with electron beams and dielectric waveguides shows that in both cases, the diffraction radiation spatial harmonics can be excited with appropriate parameters κ, β, and ε on the metal-dielectric structure (in Fig. 1 – traces 1, spread in free space). Traces 2 in Fig. 1 correspond to Cherenkov and anomalous diffraction radiation [12] regimes. These traces are concentrated in the dielectric volume and can come out through the metal-dielectric structure faces due to its total internal reflection from side surfaces. Thus, the experimental modeling method [8] (when an electromagnetic wave radiation of the electron beam space charge is modeled by surface wave radiation of a planar dielectric waveguide) is an efficient technique for new electrodynamic system modifications and research in various diffraction electronics devices.

2.1. Modeling regimes

Considering the normalized surface wave propagation velocity in a dielectric waveguide β_w, the electromagnetic wave radiation condition in free space, where only negative harmonics of diffraction radiation can exist, is

$$\frac{\kappa}{|n|+\kappa} \le \beta_w \le \frac{\kappa}{|n|-\kappa} \tag{14}$$

while in dielectric:

$$\frac{\kappa}{|n| + \kappa\sqrt{\varepsilon}} \le \beta_{\mathrm{w}} \le \frac{\kappa}{|n| - \kappa\sqrt{\varepsilon}} \tag{15}$$

The angles of electromagnetic wave radiation in free space γ_{nv} and in dielectric $\gamma_{n\varepsilon}$ for the β_{w} given parameters are defined as

$$\gamma_{nv} = \operatorname{acos}\left(\frac{1}{\beta_{\mathrm{w}}} + \frac{n}{\kappa}\right) \tag{16}$$

$$\gamma_{n\varepsilon} = -\operatorname{acos}\left(\frac{1/\beta_{\mathrm{w}} + n/\kappa}{\sqrt{\varepsilon}}\right) \tag{17}$$

here $\beta_{\mathrm{w}} = v_{\mathrm{w}}/c$ is the normalized phase velocity in the waveguide, v_{w} is the absolute phase velocity.

For parameters κ, β_{w} and ε, according to Eqs. (16) and (17), only spatial harmonics with negative indexes $n = -1, -2, -3, \ldots$ are excited in free space, and harmonics with indexes $n = 0, \pm1, \pm2, \ldots$ are excited in the dielectric. The zeros harmonic ($n = 0$) is excited at an angle $\cos(\gamma_{0\varepsilon}) = 1/(\beta_{\mathrm{w}}\varepsilon^{1/2})$ if the surface wave speed is $\varepsilon\beta_{\mathrm{w}}^2 > 1$. Therefore such a radiation can be referred to as Cherenkov radiation and the periodic structure can be considered as a shield affecting the coupling coefficient between the dielectric waveguide and the dielectric medium.

The previously described radiation regimes analysis can be performed by plotting Brillouin diagrams [13, 14] for the given values of the medium dielectric permittivity. Depending on parameters κ, β_{w} and ε, the distributed radiation source (electron beam or dielectric waveguide) excites body or surface electromagnetic waves. Brillouin diagrams were obtained by solving the following inequalities graphically:

$$\left|\frac{\eta + n}{\kappa}\right| < 1, \qquad \left|\frac{\eta + n}{\kappa}\right| < \sqrt{\varepsilon} \tag{18}$$

The diagrams contain regions limited by straight lines $\kappa = \pm(\eta + n)$, $\kappa = \pm(\eta + n)\varepsilon^{-1/2}$, which are denoted by numbers N_s^m, and define most typical cases of excitation by an electron beam (or dielectric waveguide surface wave): $N = 1$ – Cherenkov radiation; $N = 2$ – surface waves; $N = 3$ – diffraction radiation into the dielectric medium; $N = 4$ – simultaneous Cherenkov and diffraction radiations; $N = 5$ – diffraction radiation into the dielectric ($z < -a$) and into free space ($z > -a$). The subscript $s = 0, \pm1, \pm2, \ldots$ corresponds to the spatial harmonic index radiated in the dielectric; the superscript $m = -1, -2, \ldots$ corresponds to the spatial harmonic index radiated in free space.

A wide range of low loss dielectric materials is currently available on the market. It could be used for experimental modeling (materials with low dielectric constant ε such as Teflon, polystyrene, polycor) as well as for low voltage oscillators implementation based on metal-dielectric structures (materials with high dielectric constant ε

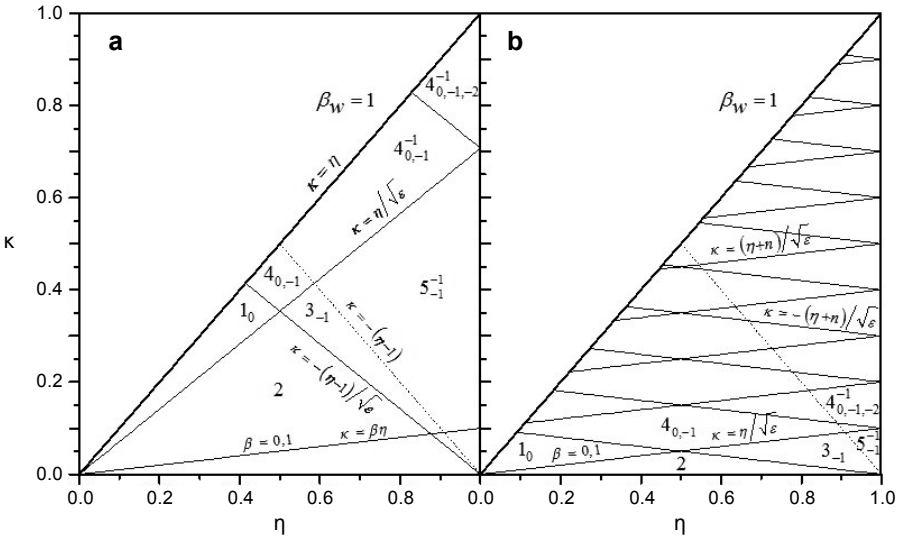

Fig. 2. An example of the Brillouin diagram for the radiation excited on the metal-dielectric structure with a dielectric permittivity of $\varepsilon = 2$ (**a**), $\varepsilon = 100$ (**b**). Solid lines – the boundary of harmonic body waves existence in the dielectric, dotted lines – the boundary of harmonic body waves existence in free space.

such as ceramics based on barium oxide and titanium oxide [15]). The diagrams of κ *vs*. $\eta = \kappa/\beta_w$ for two values $\varepsilon = 2$ and $\varepsilon = 100$ are given in Fig. 2 as an example.

The presented diagrams indicate that depending on ε, various radiation or modeling regimes can be realized by choosing parameters β_w and κ. In particular, it is possible to obtain both Cherenkov and diffraction radiation for non-relativistic electron beam and high ε (refer to zones 1_0, $4_{0,-1}$, $4^{-1}_{0,-1,-2}$ in Fig. 2**b**). In this case, the diffraction harmonics with positive indices radiate at a sharp angle. Such zones realization for a low voltage electron beam is not possible because they are located above the line $\beta_w = 0.1$ defining non-relativistic velocities of electrons. From practical point of view, zone 3_{-1} is most interesting for low voltage oscillators realization. For this zone the diffraction radiation exists only in the dielectric structure but at much lower electron velocities. Considering the specific conditions for excitation of such a spatial mode, we will refer to it as an anomalous diffraction radiation. Zone 5^{-1}_{-1} (Fig. 2**b**) is interesting for low voltage orotrons realization.

2.2. Experimental setup

The experimental setup for generalized cases modeling is presented in this work. It allows to investigate electromagnetic properties of different irregular structures (metal-dielectric structures, planar and corrugated metallic gratings and others) by a surface wave excitation using a dielectric waveguide. The setup consists of two main blocks (Fig. 3): a system for network analysis and a system for radiation characteristics measurement of the periodic structures (near field and far field characterization). Here, the structure under test is a dielectric slab 1 with a planar diffraction grating 2. The slab 1 position

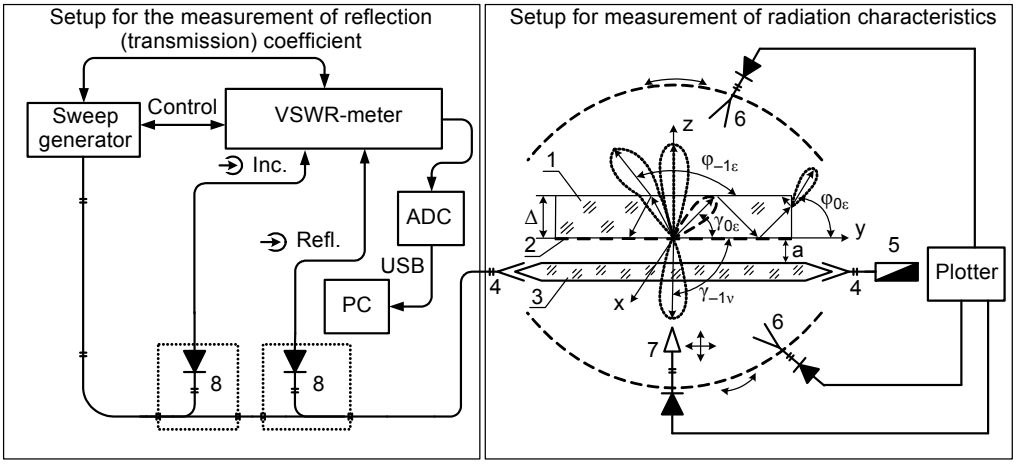

Fig. 3. Block diagram of the experimental setup.

in all three dimensions is controlled with a precision of ±0.1 mm. The dielectric waveguide 3 is connected to the system for network analysis and the matching load 5 using transitions 4 and rectangular waveguides of corresponding dimensions. As it was shown above, there are several regimes for surface waves transformation into the free space waves, which depend on the dielectric waveguide parameters and the metal-dielectric structure. The most important regimes are sketched out in Fig. 3 as radiation patterns, where γ is the radiation angle for the metal-dielectric/dielectric-waveguide structure; φ is the corresponding radiation harmonics angle in free space after propagation through the slab. In Fig. 3, x, y, z are the coordinates, Δ is the dielectric layer thickness, a = 0.4 mm is the distance between the dielectric waveguide and planar grating.

The system for radiation characteristics measurement contains two mechanically scanned horn antennas 6. The *E*-plain of the horn antennas is aligned with the vertical plane of the grating 2, and *H*-plain is aligned with the longitudinal axis of the dielectric waveguide 3. This allows the measurements in the range of $\varphi = 10°$ to $\varphi = 170°$ with accuracy $\Delta\varphi = \pm 0.25°$ in the far field, which is defined as $z \geq a_{\mathrm{m}}^2/\lambda$, where a_{m} is the antenna aperture largest dimension. During the radiation, the pattern measurement results received by the horn 6 signal are fed to the data plotter *Y* input, while port *X* is connected to the receiving horn antenna positioning system. Such an arrangement allows to acquire the radiation pattern which is then further processed on the computer. The amplitude field distribution above the radiating system is measured in the near field ($z \approx \lambda$) using the probe 7. The probe is a dielectric wedge connected to the standard waveguide using a transition. The signal from the probe 7 is detected, acquired by the data plotter, and processed on the computer. The probe size is approximately 0.1λ to 0.2λ, which is chosen to minimize the parasitic influence on the measured field. The positioning system accuracy for the near field probe is ±0.1 mm.

The system for network analysis (Fig. 3) consists of an SWR indicator, directional couplers 8 with detectors connected to the indicator corresponding ports. The setup

allows to measure the transmission coefficient or SWR in the desired frequency range depending on directional couplers connection. The measured data is then digitized with an analog-to-digital converter (ADC) and stored on a computer (PC) via USB interface for further processing. The constant power level at the structure input under test is achieved using an automatic power control circuit. The reflections from the dielectric waveguide output are minimized by terminating it with a matched load 5. This matched load is substituted with a power meter if the absolute power measurements are required.

2.3. Experimental modeling

The described experimental setup has been realized at frequency range from 53 to 80 GHz. The corresponding SWR meter has been used with a waveguide cross-section 3.6×1.8 mm^2. The dielectric waveguides made of Teflon (cross-section 5.2×2.6 mm^2) and polystyrene (cross-section 7.2×3.8 mm^2) allowed to achieve surface waves with β_w from 0.6 to 0.8 and excite three spatial harmonics 1_0, 3_{-1} and $4^{-1}_{0,-1,-2}$ (refer to Brillouin diagram in Fig. 2**a**) on the metal-dielectric structure. The metal-dielectric periodic structure samples have been fabricated using Teflon slab with a cross-section 54×60 mm^2 for three values of Δ: $\Delta_1 \approx \lambda/4$, $\Delta_2 \approx \lambda$, and $\Delta_3 \approx 4\lambda$. The chosen cross-section minimizes the multiple reflections influence from the ends on structure radiation characteristics. The planar diffraction grating has been fabricated using a photolithography process with ±0.01 mm precision. The employed metal-dielectric structure parameters for three fundamental free-space wave excitation regimes are given in the Table, where parameter $u = \cos(\pi d/l)$ is a grating filling factor. It was chosen according to intensity maximums of the main radiated spatial harmonics in the investigated zones.

T a b l e. Metal-dielectric structures parameters.

Wave indices	l [mm]	d [mm]	κ	u	β_w
$n = 0$ (in dielectric)	1.17	0.39	0.30	+0.5	0.788
$n = 0, -1, -2$ (in dielectric) $n = -1$ (in free space)	3.07	1.535	0.79	0	0.788
n = –1 (in dielectric)	1.36	1.084	0.35	–0.8	0.598

The experimentally obtained data has been compared with the simulated data. Simulations have been done using CST Microwave Studio. The measured data indicates that the maximum directivity is achieved for prism thickness exceeding a wavelength. Typical normalized radiation patterns (P/P_{max}, where P_{max} is the maximum power of the radiated harmonic with index n) of metal-dielectric structures having $\Delta = \lambda$ parameters, which are given in the Table, are presented in Fig. 4.

As one can see from the data presented in Fig. 4**a**, the radiation patterns for Cherenkov ($n = 0$) and anomalous diffraction ($n = -1$) radiation (curve 1, solid line) contain one lobe which agrees with the data obtained using finite-difference simulation (curve 2, dotted line). For the diffraction-Cherenkov radiation regime (zone $4^{-1}_{0,-1,-2}$ in Fig. 4**b**) Cherenkov harmonics and diffraction harmonics, which are radiated in free

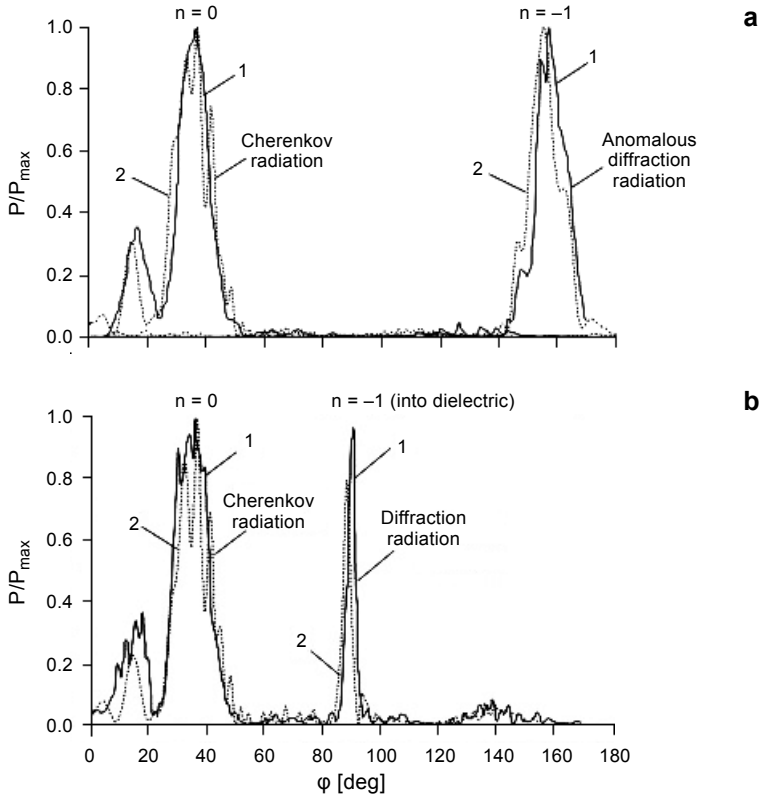

Fig. 4. Experimentally (curve 1) and numerically (curve 2) obtained metal-dielectric structure radiation patterns; Cherenkov and anomalous diffraction regimes (**a**), Cherenkov diffraction regime (**b**).

space through the dielectric (minus first harmonics), dominate and have approximately the same intensity. This fact is caused by a corresponding value of the grate filling factor $u \approx 0$, when harmonics with $n = -1$ have maximum energy density. Diffraction harmonic intensity with $n = -2$ ($\varphi_{-2\varepsilon} \approx 140°$) is lower than the main harmonic intensity by order of magnitude and can be seen in Fig. 4**b** as a background radiation. The discrepancy between the measured and simulated data can be explained by technological imperfections in metal-dielectric structure fabrication, as well as by the theoretical model inaccuracy, which assumes that the metal is perfectly conducting.

2.4. Practical applications

The described metal-dielectric structure properties allow to analyze its implementation perspectives. In particular, in various vacuum tube devices as well as electromagnetic components in millimeter wave and terahertz range, where fabrication can be done using modern micro-fabrication processes [16, 17]. Figure 5**a** illustrates an open resonator complex system with the metal-dielectric structure, which is formed of spherical mirror with energy output and plane mirror with reflecting grating [18].

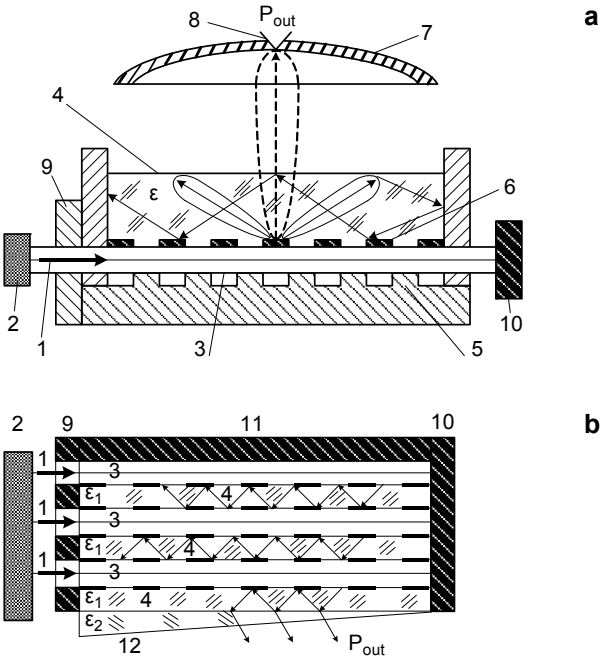

Fig. 5. Schematic view of low voltage vacuum devices employing multi-coupled metal-dielectric structures: diffraction-Cherenkov generator (**a**), backward wave tube (**b**). Here 1 – the electron beam, 2 – the electron gun, 3 – the transit channel, 4 – the planar periodic metal-dielectric structure, 5 – the slow-wave structure, 6 – the ribbon grating, 7 – the movable mirror, 8 – the coupling slot, 9 – the anode, 10 – the collector, 11 – the mirror (screen), and 12 – the energy output.

The metal-dielectric structure made as a dielectric resonator is placed between the open resonator mirrors. Such electrodynamic system is basic in fabrication of diffraction-Cherenkov generators. Possible regimes of the diffraction-Cherenkov radiation excitation by a distributed radiation source located nearby the dielectric prism edge with the strip diffraction grating have been analyzed in Section 2 and presented in Fig. 5**a**. Modeling of experiment showed that introducing the above-described metal-dielectric structures into an open resonator causes new electrodynamic properties of such system [4]: energy attenuation regimes in the open resonator, regimes of increasing oscillations amplitude and its Q factor, oscillation selection can be realized with changing metal-dielectric structure parameters.

Such systems further research allowed to propose and prove concrete diffraction electronics devices with space-developed resonator structures. Specifically, generalized diffraction-Cherenkov generator scheme is presented in Fig. 5**a**. Electron beam 1 is formed by the gun 2 and moves along the channel 3, which is shaped by adjoining dielectric resonator 4 surfaces and slow-wave structure (diffraction grating) 5. This slow-wave structure is located in the central part of the immovable mirror. Movable mirror 7 with coupling slot 8 is used to extract the energy. Electrons interact with surface slow wave field of the slow-wave structure 5. They are modulated in charge density

and give their energy to open resonator volume and to dielectric 4 as well. The similar concept to the low voltage backward wave tubes with several parallel slow-wave structures [19, 20] is presented in Fig. 5. The backward-wave tube diagram based on an anomalous diffraction radiation for a metal-dielectric structure (zone 3_{-1} in Fig. 2**b**) is shown in Fig. 5**b**. The arrows show the radiation wave direction from the metal-dielectric structure. Figure 5 shows that the diffraction-grating/metal-dielectric structure or parallel metal-dielectric structures at acceleration voltages $U \approx 1000$ V and $\varepsilon_r = 100$ (ceramics based on titanium oxide [15]) can be realized for a wavelength range from 1 to 0.1 mm and periods l from 64 to 4 μm. Currently the fabrication technology for such structures is mature and has been used for multiple parallel slow-wave structures fabrication in backward-wave tubes. The fabrication technologies include electro-erosion machining, cold forming, photolithography, electron and X-ray lithography, vacuum and plasma deposition. The slow-wave structures fabrication of vacuum electron tubes requiring nanoscale precision is performed by ion beam lithography in combination with nanoforming [21]. In order to realize the described devices in submillimeter and infrared wave ranges, an electron beam should be as thin as 0.04 mm. Such electron beams practical realization is possible using an array type [22] or slot type L-cathode [23], which allow for uniformly distributed and stable electron emission with high current density at comparatively low field intensity.

3. Conclusions

In this work, we have developed and evaluated a generalized approach to experimental modeling of Cherenkov radiation and diffraction radiation on periodic metal-dielectric structures in a millimeter wavelength range. The approach and experimental setup were used to estimate electromagnetic properties of such structures avoiding heavy computations, which are often not feasible. It can also be concluded that the developed setup is suitable and has a good accuracy for predicting performance of different complicated structures. The experimental data have been compared with the numerically obtained data. Apart from that, the approach has some drawbacks. For example the radiation power cannot be predicted as well as the electron efficiency and nonlinear effects, if the electron beam in the system is not considered. The performance estimation and realizability with traditional and new technological processes for planar metal-dielectric structures are discussed. The structures have a great potential benefit for new vacuum tubes modifications such as orotrons and backward wave oscillators in a submillimeter and infrared wave range.

Acknowledgements – The authors would like to thank Lundbeck Foundation and Ukrainian governmental program No. 0115U000690 for partial support of the activities.

References

[1] Whitaker J., *Power Vacuum Tubes Handbook*, 3rd Ed., Technical Press, Morgan Hill, California, 2012.

[2] Savich M., *High power tube solid-state laser with zigzag propagation of pump and laser beam*, Proceedings of SPIE 9342, 2015, article ID 934216.

[3] http://vadiodes.com
[4] VOROB'YOV G.S., PETROVSKII M.V., KRIVETS A.S., *Possible applications of quasioptical open resonant metal-dielectric structures in EHF electronics*, Radioelectronics and Communications Systems 49(7), 2006, pp. 38–42.
[5] SAUTBEKOV S., SIRENKO K., SIRENKO Y., VERTIY A., YEVDOKYMOV A., *Diffraction radiation phenomena: physical analysis and applications*, [In] Y. Sirenko, L. Velychko [Eds.], *Electromagnetic Waves in Complex Systems*, Springer Series on Atomic, Optical, and Plasma Physics, Vol. 91, 2016, pp. 387–442.
[6] LIN ZHAO, HUI XIE, LONGGEN ZHENG, *Electromagnetic properties analysis of multilayered structure of metal-dielectric nanofilms*, Advanced Science Letters 5(1), 2012, pp. 64–68.
[7] VOROBYOV G.S., TZVYK A.I., PUSHKARYOV K.A., MAKEYEV O.S., *Scattering of electron stream waves on metal-dielectric structures*, Journal of Infrared, Millimeter, and Terahertz Waves 17(10), 1996, pp. 1761–1768.
[8] VOROBJEV G.S., ZHURBA V.O., PETROVSKY M.V., RYBALKO A.A., *A setup for measuring spatial and waveguide characteristics of periodic metal-dielectric structures*, Instruments and Experimental Techniques 53(4), 2010, pp. 536–538.
[9] KRIVETS A.S., PETROVSKYI M.V., TSVYK A.I., SHMAT'KO A.A., *The Smith–Pursell effect amplification of the electromagnetic waves in an open waveguide with a metal-dielectric layer*, Telecommunications and Radio Engineering 59(10–12), 2003, pp. 80–92.
[10] GINZBURG M.S., ZOTOVA I.V., KOVALEV N.F., SERGEEV A.S., *Theory of stimulated Cherenkov emission from sheet relativistic electron beams in a uniform isotropic dielectric medium*, Journal of Experimental and Theoretical Physics **77**, 1993, pp. 893–900.
[11] TAMIR T. [Ed.], *Integrated Optics*, Springer-Verlag, Berlin, Heidelberg GmbH, 1975.
[12] TSVYK A.I., TSVYK L.I., *Phenomenon of anomalous diffraction radiation in the metal-dielectric grating*, 12th International Conference Microwave and Telecommunication Technology, Sevastopol, Ukraine, September 9–13, 2002, Weber, pp. 194–195.
[13] BACCARELLI P., PAULOTTO S., JACKSON D.R., OLINER A.A., *A new Brillouin dispersion diagram for 1-D periodic printed structures*, IEEE Transactions on Microwave Theory and Techniques 55(7), 2007, pp. 1484–1495.
[14] BRILLOUIN L., *Wave Propagation in Periodic Structures*, McGraw–Hill, New York, NY, 1946.
[15] NENASHEVA E.A., TRUBITSYNA O.N., KARTENKO N.F., USOV O.A., *Ceramic materials for use in microwave electronics*, Physics of the Solid State 41(5), 1999, pp. 799–801.
[16] VOROBYOV G.S., PONOMAREV A.G., PONOMARYOVA A.A., DROZDENKO A.A., RYBALKO A.A., *Application of focused charge-particle beams in manufacturing of nanocomponents*, Telecommunications and Radio Engineering 69(4), 2010, pp. 355–365.
[17] BYEON K.-J., LEE H., *Recent progress in direct patterning technologies based on nano-imprint lithography*, The European Physical Journal Applied Physics 59(1), 2012, article ID 10001.
[18] RYBALKO A.A., RUBAN A.I., VOROB'EV G.S., DOROSHENKO D.YU., *A setup for measuring characteristics of microwave electric vacuum devices with open resonance structures*, Instruments and Experimental Techniques 58(4), 2015, pp. 515–519.
[19] ZHURBENKO V. [Ed.], *Electromagnetic Waves*, InTech, 2011.
[20] BRATMAN V.L., DUMESH B.S., FEDOTOV A.E., MAKHALOV P.B., MOVSHEVICH B.Z., RUSIN F.S., *Terahertz orotrons and oromultipliers*, IEEE Transactions on Plasma Science 38(6), 2010, pp. 1466–1471.
[21] WATT F., BETTIOL A.A., VAN KAN J.A., TEO E.J., BREESE M.B.H., *Ion beam lithography and nanofabrication: a review*, International Journal of Nanoscience 4(3), 2005, pp. 269–286.
[22] IONOV A.N., POPOV E.O., SVETLICHNYI V.M., PASHKEVICH A.A., *Field electron emission from flat metal cathodes covered by thin polymer films*, Technical Physics Letters 30(7), 2004, pp. 566–568.
[23] BELOUSOV YE.V., ZAVERTANNIY V.V., NESTERENKO A.V., *The diode slit L-cathode electron gun*, Telecommunications and Radio Engineering 66(1), 2007, pp. 69–78.

Received January 16, 2017
in revised form May 3, 2017